In Vitro Toxicity Assessment of Amphiphillic Polymer-Coated CdSe/ZnS Quantum Dots in Two Human Liver Cell Models

Wesley E. Smith,[†] Jessica Brownell,[‡] Collin C. White,[†] Zahra Afsharinejad,[†] Jesse Tsai,[†] Xiaoge Hu,[§] Stephen J. Polyak,[‡] Xiaohu Gao,[§] Terrance J. Kavanagh,[†] and David L. Eaton[†,*]

Departments of [†]Environmental & Occupational Health Sciences, [‡]Laboratory Medicine, and [§]Bioengineering, University of Washington, Seattle, Washington 98195, United States

Semiconductor quantum dots (Qdots) are a distinct category of nanotechnology that has potential for medical applications, in addition to other industrial applications. Compared to fluorescent proteins and organic dyes, Qdots offer greater brightness and photostability, tunable emission from visible to infrared wavelengths, and large absorption coefficients across a broad spectral range. This allows for highly specific, quantitative optical imaging and multiplex assays. Recent studies from our group,[1,2] as well as others,[3] have shown that nanometer-sized Qdots can be covalently linked to a variety of biomolecules, such as antibodies, DNA, and RNA for use as addressable fluorescent probes. For example, we have conjugated antibodies targeting PSMA (prostate-specific membrane antigen) to CdSe/ZnS core/shell Qdots (emission 640 nm) for simultaneous imaging and targeting prostate tumors in mouse models,[4] and more recently, we have developed silica—polymer dual-encapsulated Qdots which are stable in a wide range of chemical conditions.[1] A recent study by Ling *et al.*[5] reported no adverse events after intravenous dosing of rhesus macaques with phospholipid-encapsulated CdSe/CdS/ZnS Qdots, further illustrating the potential promise and apparent safety of this technology.

However, while this technology shows much promise, the semiconductor crystalline core of Qdots is generally made from toxic heavy metals in groups II—VI and III—V of the chemical periodic table, including Cd, Se, Te, and Hg. It is therefore important to investigate the disposition of Qdots in an attempt to understand and mitigate any possible toxicity that may be associated

ABSTRACT Semiconductor quantum dots (Qdots) are a promising new technology with benefits in the areas of medical diagnostics and therapeutics. Qdots generally consist of a semiconductor core, capping shell, and surface coating. The semiconductor core of Qdots is often composed of group II and VI metals (*e.g.*, Cd, Se, Te, Hg) that are known to have toxic properties. Various surface coatings have been shown to stabilize Qdots and thus shield cells from the toxic properties of their core elements. In this study, HepG2 cells and primary human liver (PHL) cells were chosen as *in vitro* tissue culture models of human liver to examine the possible adverse effects of tri-*n*-octylphosphine oxide, poly(maleic anhydride-*alt*-1-tetradecene) copolymer (TOPO-PMAT)-coated CdSe/ZnS Qdots (TOPO-PMAT Qdots). The TOPO-PMAT coating is desirable for increasing aqueous solubility and ease of conjugation to targeting moieties (*e.g.*, aptamers and peptides). HepG2 cells avidly incorporated these TOPO-PMAT Qdots into subcellular vesicles. However, PHL cells did not efficiently take up TOPO-PMAT Qdots, but nonparenchymal cells did (especially Kupffer cells). No acute toxicity or morphological changes were noted in either system at the exposure levels used (up to 40 nM). However, cellular stress markers and pro-inflammatory cytokines/chemokines were increased in the PHL cell cultures, suggesting that TOPO-PMAT Qdots are not likely to cause acute cytotoxicity in the liver but may elicit inflammation/hepatitis, demonstrating the importance of relevant preclinical safety models. Thus, further *in vivo* studies are warranted to ensure that TOPO-PMAT-coated Qdots used in biomedical applications do not induce inflammatory responses as a consequence of hepatic uptake.
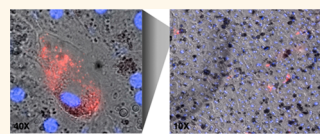
KEYWORDS: human liver · hepatocytes · nanotoxicology · quantum dots · HepG2 cells

with exposure. Previously reported studies utilizing Qdots with a CdSe core have presented conflicting toxicity results. Derfus *et al.*[6] reported that Qdot toxicity is due primarily to the release of Cd+ ions, rather than the surface properties of Qdots. These results were further substantiated in another study.[7] Additionally, Su *et al.*[8,9] found that various CdTe/CdSe/ZnS core-structured

Qdots formed by aqueous synthesis were highly toxic in a variety of cell lines, and that the toxicity was related to release of Cd ions, which could be ameliorated with the addition of a ZnS shell. While a ZnS shell may help ameliorate toxicity due to release of Cd atoms, surface coatings used to improve biocompatibility also hold potential for toxicity. For example, a study by Shiohara and colleagues[10] concluded that cytotoxicity was predicted primarily by Qdot surface properties. Thus, a variety of cellular responses in different cell types have been observed with Qdots of differing surface properties and coatings. These differences are likely due to the particular cell types and *in vitro* culture methods used in these studies, as well as to differences in surface properties of the Qdots.[7,11]

In vivo, Fischer and co-workers have previously shown that up to 99% of an intravenous dose of bovine serum albumin (BSA)-conjugated Qdots was found within the liver of Sprague–Dawley rats 90 min after administration.[12] Furthermore, it was also shown that these Qdots were sequestered primarily by macrophages (Kupffer cells) within the liver.[12] Another study showed the importance of Kupffer cells in the sequestration of epidermal growth factor (EGF)-conjugated Qdots in rat liver since pre-administration of gadolinium chloride (a Kupffer cell-specific toxicant) was able to severely diminish retention of these Qdots to the liver.[13] These studies suggest that the liver is a primary site of Qdot accumulation following intravenous exposure.

Cell culture models are necessary for preclinical safety assessment during the development of biomedical nanoparticles. The biological relevance of the model system must be accounted for to generate a reliable prediction of *in vivo* responses. Primary human hepatocytes are regarded as the "gold standard" for preclinical safety testing of therapeutic molecules.[14] Culturing these cells in various "sandwich culture" formats allows for the maintenance of many liver-specific functions.[15] This *in vitro* system has been shown to maintain gene expression levels similar to those *in vivo* with both primary human[16] and rat[17] hepatocyte cultures. However, the utility of this system has not been established for testing of nanoparticles. Because the liver is likely one of the primary sites of uptake after intravenous administration, we chose to analyze the disposition of multifunctional Qdots in primary human liver (PHL) cell cultures, utilizing the transformed human liver cell line HepG2 as a comparison. Specifically, we investigated the effects of tri-*n*-octylphosphine oxide, poly(maleic anhydride-*alt*-1-tetradecene) copolymer (TOPO-PMAT)-coated CdSe/ZnS Qdots on cultured HepG2 cells and PHL cells.

RESULTS

Characterization of TOPO-PAMT Qdots. Characterization data used in all of the experiments reported in this study are detailed in Figure 1. Qdots used in this study
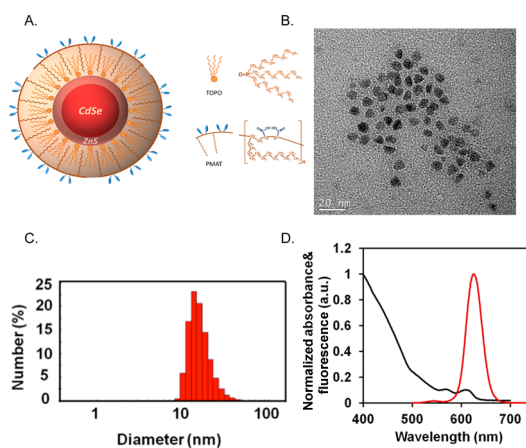

Figure 1. Particle characterization.

contain a CdSe core with a ZnS shell and a polymer (TOPO-MAT) coating (Figure 1A). TEM evaluation of the stock solution of Qdots revealed individual nanoparticles (Figure 1B) with a mean hydrodynamic diameter of 12.7 ± 0.5 nM (Figure 1C) and peak fluorescence emission spectra of 620 nm (Figure 1D). TOPO-PMAT Qdots showed very little agglomeration in the cell culture conditions utilized (S1).

Uptake of TOPO-PMAT Qdots in HepG2 and PHL Cells. To quantify the amount of TOPO-PMAT Qdot uptake in HepG2 and PHL cultures, the cells were exposed to a range of concentrations (0–40 nM). Both culture systems showed TOPO-PMAT Qdot sequestration in a dose-dependent manner at 24 h. Qdot-specific fluorescence intensity was normalized to cell count using Hoechst nuclear staining (Figure 2A,B). The fluorescence signal attributable to TOPO-PMAT Qdots in PHL cell cultures appeared to be saturated at lower concentrations *versus* that obtained for HepG2 cell cultures (Figure 2C). Visually, TOPO-PMAT Qdots were present in a subpopulation of cells within the PHL cell cultures (Figure 2A), whereas nearly all HepG2 cells showed some uptake (Figure 2B).

Effect of TOPO-PMAT Qdots on Cellular Viability and Markers of Cellular Stress. To investigate the effect of TOPO-PMAT Qdots on cell viability, cultures were exposed to a range of concentrations and examined for their ability to carry out the reduction of MTT to formazan. Administration of TOPO-PMAT Qdots to either culture system did not affect cell viability at the concentrations tested over a period of 24–72 h (Figure 3A, 48 and 72 h data not shown).

To determine if TOPO-PMAT Qdots were causing sublethal changes in cell function, several markers of cellular stress were examined. HepG2 and PHL cells were analyzed for total GSH content (Figure 3B). GSH was significantly increased over controls in PHL cells exposed to TOPO-PMAT Qdots at 5, 10, 20, and 40 nM with values of 131, 132 150, and 147% of control, respectively. In contrast, HepG2 cultures showed no dose-related effect on GSH levels.
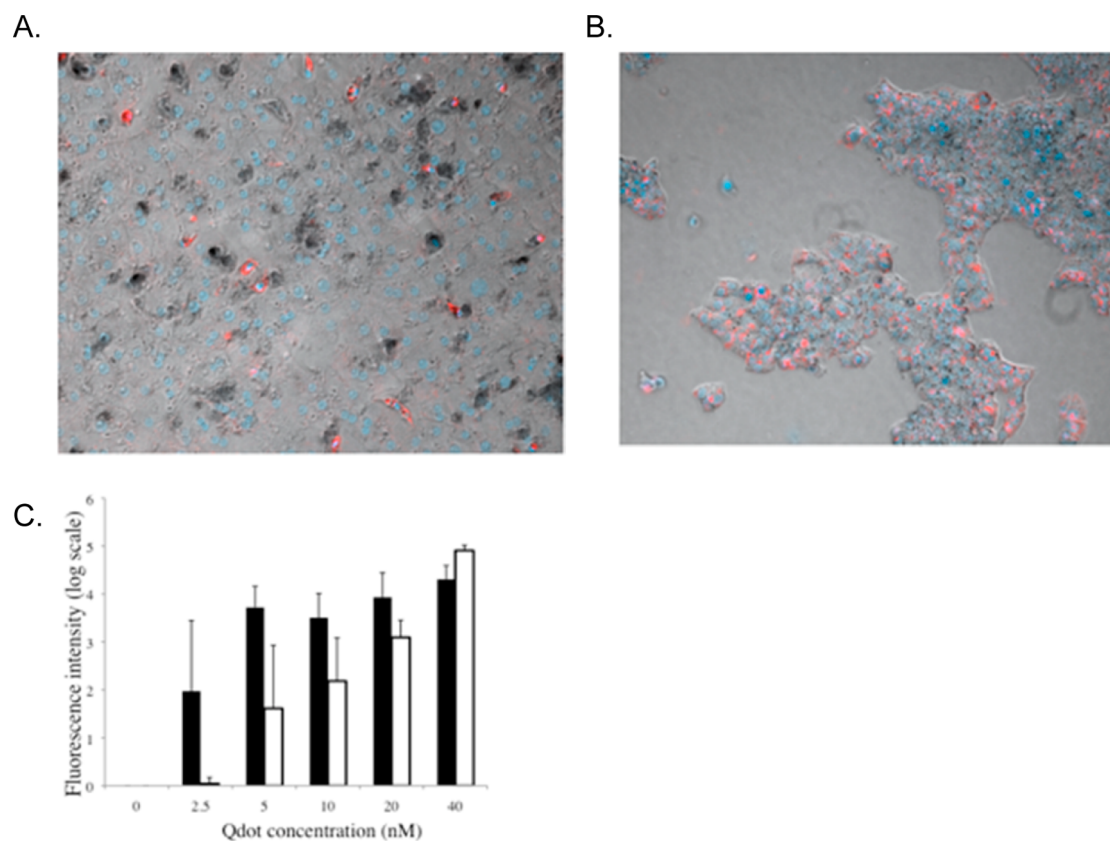
A.

B.

C.

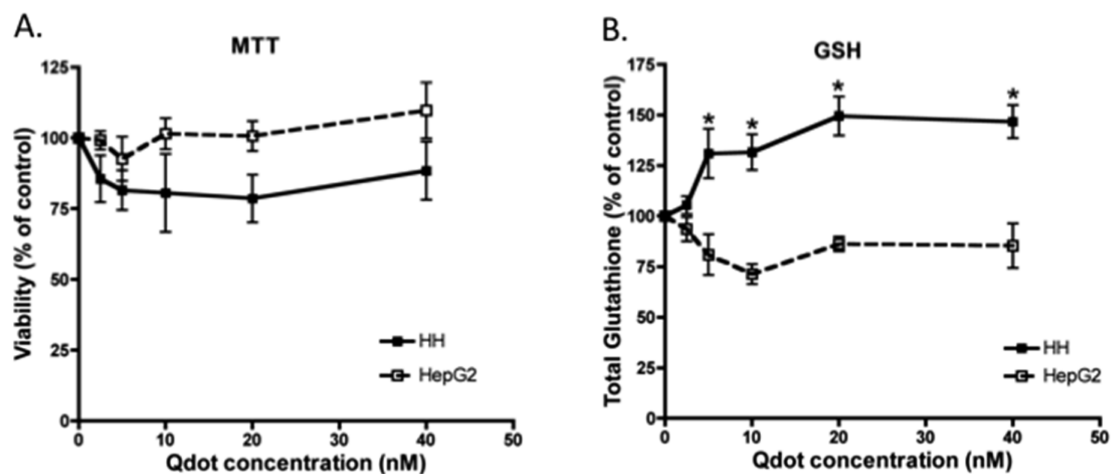**Figure 2. Quantum dot uptake.**

A.

B.

Figure 3. Effect of Qdots on cellular viability and glutathione content.

The mRNA expression of four oxidative stress responsive genes (*MT1A*, *HMOX1*, *GCLC*, and *GCLM*) and their corresponding protein levels were measured in both HepG2 and PHL cell cultures (Figure 4A−D The levels of *GCLC* and *GCLM* mRNA were relatively unaffected in HepG2 cultures (Figure 4A,B). However, the mRNA expression of GCLC, and to a lesser extent GCLM, was downregulated in PHL cell cultures, in spite of the increased levels of GSH detected in these cells (Figure 3B). *HMOX1* mRNA expression was maximally increased 3-fold at 10 nM TOPO-PMAT Qdot concentration (Figure 4C).

significant changes were noted in *HMOX1* mRNA levels in HepG2 cultures (Figure 4C). *MT1A* mRNA expression was similar in both culture systems (Figure 4D). To address the possibility that small traces of Cd may either be present or leaching from the TOPO-PMAT Qdots, we measured the residual amounts of Cd in medium containing a 40 nM concentration of Qdots after removal by centrifugation. The remaining levels after centrifugation were 23.7 and 60.1 nM in WEM and MEMα, respectively.

To more thoroughly investigate the cellular response to TOPO-PMAT Qdots of these cellular stress
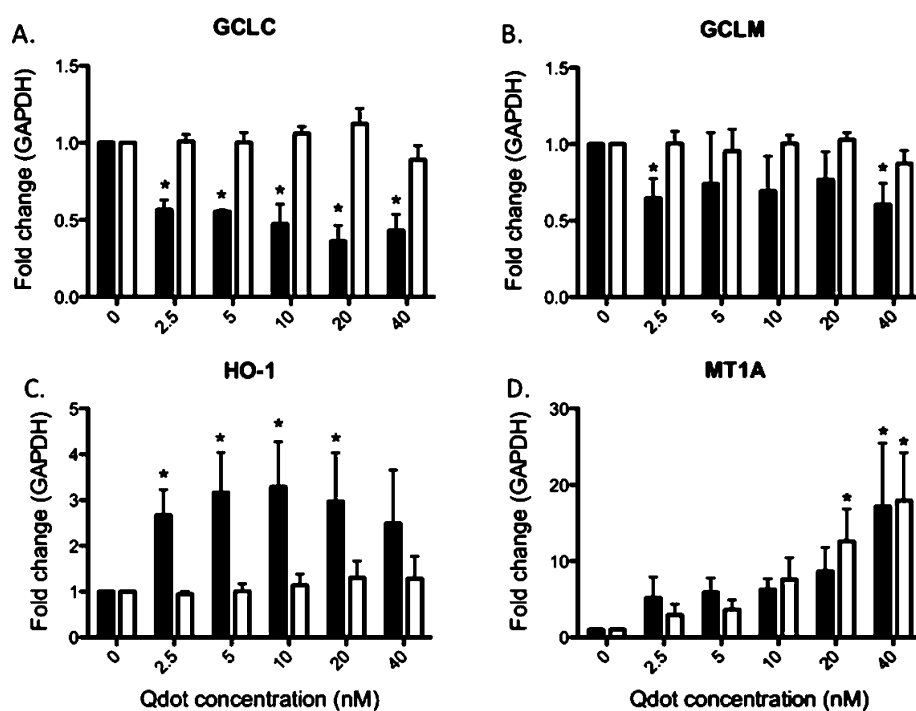
Figure 4. Changes in mRNA levels after exposure to Qdots.

markers, GCLC, GCLM, and HMOX1 protein levels were examined using Western immunoblotting (Figure 5). HMOX1 protein levels appeared to be increased in a dose-dependent manner in both cell culture models but were not statistically significant (Figure 5C). GCLC protein levels appeared to be down-regulated after 24 h of treatment with TOPO-PMAT Qdots in PHL cell cultures, while GCLM was unaffected (Figure 5A,B).

Pro-inflammatory Effects of TOPO-PMAT Qdots. Because the liver is often involved in systemic immune response,[18] we investigated the potential of TOPO-PMAT Qdots to elicit an inflammatory response in both HepG2 and PHL cell cultures. The mRNA levels of several pro-inflammatory cytokines/chemokines known to play a role in liver pathologies were measured by qRT-PCR (Figure 6A−D). TNFα, CXCL8, CCL4, and CXCL10 were measured after 24 h of exposure to TOPO-PMAT Qdots. Exposure of HepG2 cells to TOPO-PMAT Qdots resulted in very little change in mRNA levels for these pro-inflammatory cytokines/chemokines. However, there were marked increases in CXCL8 and CCL4 mRNA levels (3.3-fold and 5.5-fold, respectively) in the PHL cells (Figure 6B,C). TNFα and CXCL10 were not significantly affected by Qdot exposure in PHL cells (Figure 6A,D).

To determine if these changes in mRNA were also reflected in changes in protein, we measured the levels of these pro-inflammatory cytokines/chemokines in media collected after 24 h of exposure to Qdots (Figure 7). The levels of CXCL8, CCL4, and CXCL10 were increased across all doses in PHL cultures, while TNFα was only detectable at low levels (Figure 7A−C).

No changes in cytokine or chemokine levels were evident after Qdot exposure in HepG2 cells (Figure 7).

DISCUSSION

In this study, we have found that cultured HepG2 cells and PHL cells sequester TOPO-PMAT Qdots in a dose-dependent manner with no overt cytotoxicity after 24 h. The TOPO-PMAT coating appears to protect cells from acute toxicity due to Cd^{2+} ions, as reported by others for various uncoated, Cd-containing Qdot cores.[8,9,11,19] However, these particles cause increases in total glutathione levels and HMOX and MT1A expression in PHL cell cultures. HepG2 cells were minimally responsive to Qdots, showing only changes in MT1A mRNA expression but no response in the other stress response indicators nor in pro-inflammatory signaling molecules. PHL cell cultures responded with robust increases in CCL4 and CXCL8 mRNA expression and protein levels. Additionally, CXCL10 protein, but not mRNA, was increased after exposure. These results suggest the need for more thorough characterization of liver cell pro-inflammatory responses in order to avoid possible bystander liver injury due to inflammation.

Metallothionein was the only gene with increased expression in both culture systems. Increased (MT1) expression is acknowledged as a marker of cellular stress induced by heavy metals, including cadmium.[20] As mentioned in the Results, we measured the residual amounts of Cd by ICP-MS in medium containing 40 nM of TOPO-PMAT Qdots subsequent to centrifugation. The remaining levels after centrifugation were 23.7 and 60.1 nM in WEM and MEMα, respectively.
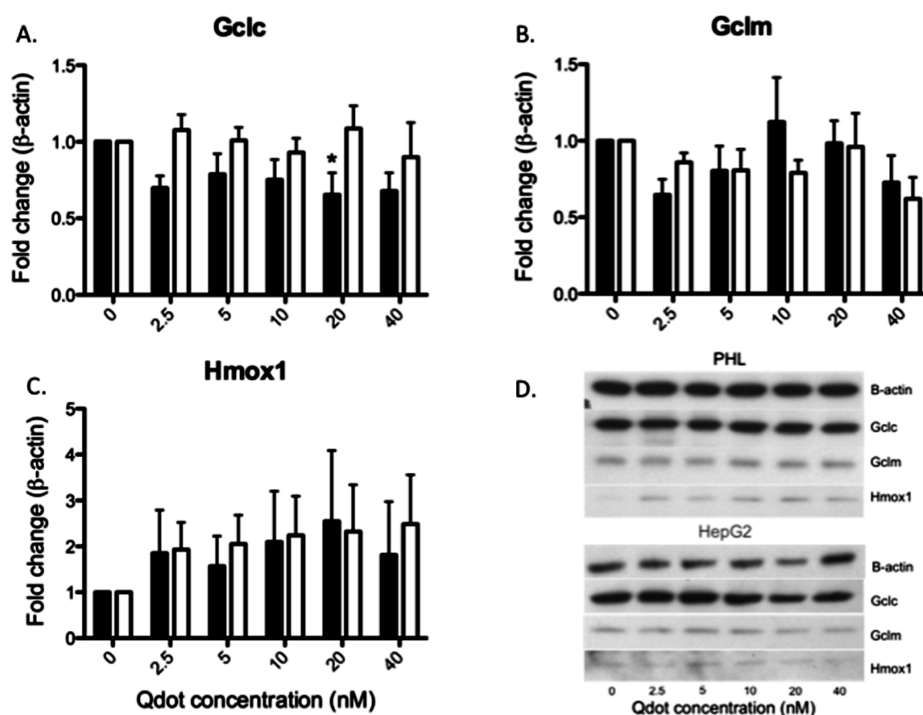
Figure 5. Expression of cellular stress response proteins after exposure to Qdots.
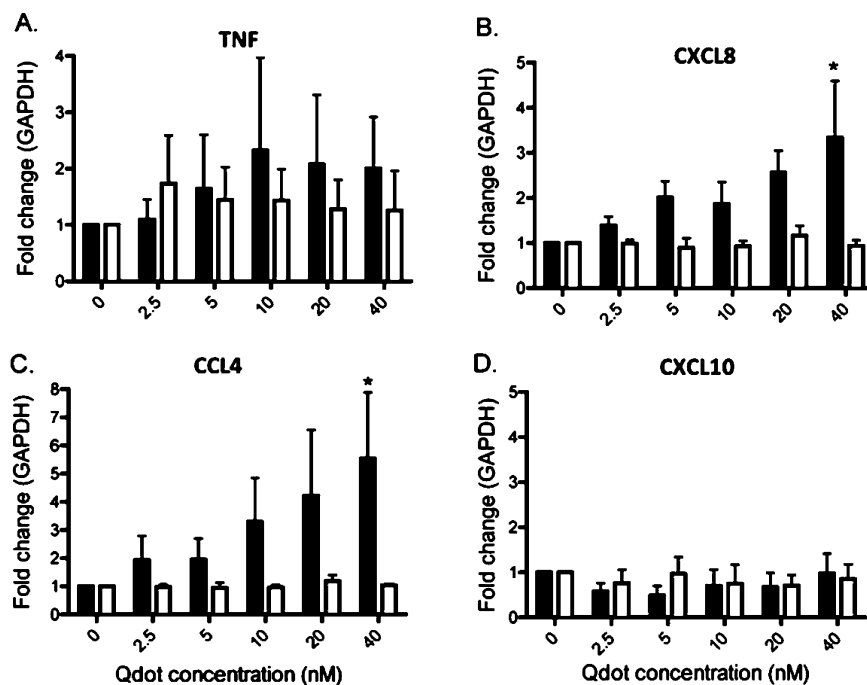

Figure 6. Changes in mRNA levels of pro-inflammatory genes after exposure to Qdots.

The calculated amount of Cd in a 40 nM concentration of TOPO-PMAT Qdots is approximately 140 μM. Previous studies have reported that 6 μM CdCl$_2$ induced *MT1* in HepG2 cells approximately 50-fold.[21,22] Given that the concentration of Cd^{2+} present in media was 100-fold lower, it is unlikely this was a substantial contributor to *MT1* induction in these experiments, suggesting a different mechanism.

The concentration of the intracellular antioxidant, glutathione (GSH), was significantly increased in PHL cultures after exposure to TOPO-PMAT Qdots. Glutathione has been shown to be important in Cd-induced toxicity.[23] Glutamate cysteine ligase (GCL) is the rate-limiting enzyme for glutathione synthesis in mammalian cells and is composed of catalytic (GCLC) and modifier (GCLM) subunits. Interestingly, TOPO-PMAT
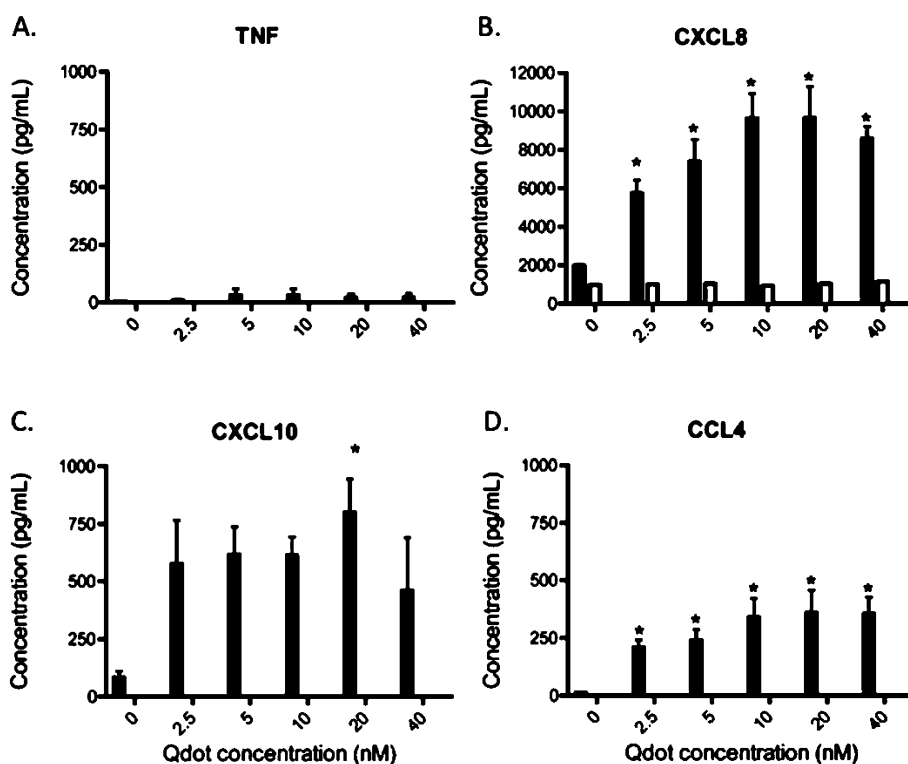
Figure 7. Expression of pro-inflammatory cytokines after Qdot exposure.

Qdot-exposed PHL cultures exhibited a significantly increased level of GSH, while HepG2 cultures show slightly decreased levels. The mRNA and protein levels of GCLC are decreased in Qdot-exposed cultures, and the levels of GCLM mRNA appear to be slightly decreased in PHL cultures. Both mRNA and protein are relatively unaffected in HepG2 cultures. The discrepancy between increased total GSH levels and decreased mRNA expression and protein is suggestive of a post-translational or biochemical mechanism. Previously, we reported similar results in a coculture system of RAW264.7 and SVEC4-10 in response to diesel exhaust particulate exposure.[24] This finding may be due to oxidative stress increasing the formation of GCL holoenzyme, resulting in more efficient generation of the dipeptide and glutathione synthesis intermediate γ-glutamyl cysteine.[25]

HMOX1 is responsible for the degradation of heme to carbon monoxide (CO), biliverdin, and free iron. These products have been shown to have antioxidant and anti-inflammatory effects.[26] HMOX1 mRNA expression is significantly increased at all doses of TOPO-PMAT Qdot treatment with only a slight increase at higher concentrations in HepG2 cells. A trend toward increased protein expression of HMOX1 is evident in both culture systems, suggesting there may be post-transcriptional events affecting the ultimate translation of HMOX1 mRNA to protein. A previous report by our group identified HMOX1 as a sensitive biomarker to TOPO-PMAT Qdots.[27]

There is also evidence to suggest that HMOX1 plays a role in reducing pro-inflammatory effects in response to toxic insult.[28] Our results show robust increases in mRNA and protein levels for several pro-inflammatory cytokines. On the basis of our finding that TOPO-PMAT Qdots are sequestered in a subpopulation of cells, most likely Kupffer cells, an increase in inflammatory cytokines is not unexpected. Multiple studies have shown the sequestration of intravenously administered Qdots in Kupffer cells within the liver. Fischer et al.[29] reported an increase in pro-inflammatory signaling (TNFα and IL-6) after exposure of rats to Qdots (PEG and BSA-coated), but they did not find an increase in IL-1β. These results differ from what we found, possibly due to either species or nanoparticle differences.

The pro-inflammatory cytokine CXCL8 was chosen for analysis due to its role in the response to infectious agents. CXCL8 is known as a potent neutrophil chemoattractant and has been shown to be elevated in individuals with chronic liver diseases.[22] Our results demonstrate a dose-dependent increase in CXCL8 mRNA and a corresponding increase in CXCL8 protein at all doses of PMAT-TOPO Qdots in PHL cultures. In contrast, HepG2 cultures showed no change in either CXCL8 mRNA or protein. This suggests that Kupffer cells are most likely responsible, directly or indirectly, for the release of CXCL8. This study does not account for responses that may originate from outside of the liver in vivo, such as recruitment of extrahepatic monocytes/macrophages into the liver.

IFN inducible protein 10 (CXCL10) is up-regulated in autoimmune hepatitis as well as chronic HBV and HCV. It is released as a soluble factor by hepatocytes near inflamed lobular regions and induces a type I immune response by activating the CXCR3 receptor on CD4+T_H1, CD8+T_c, and NK cells.[30] CXCL10 has also been shown to be involved in liver fibrosis by inhibiting NK cell inactivation of hepatic stellate cells (HSCs).[31] Exposure to Qdots results in an increase of CXCL10 protein after 24 h in PHL cultures with no concomitant increase in mRNA and no response in HepG2 cultures. Again, this is suggestive of Kupffer cells playing a role in inflammatory response in PHL cultures. Kupffer cells are generally present in these cultures at around 1% of the total cell population as measured by flow cytometry (data not shown) and thus are unlikely to contribute significantly to the amount of mRNA expression.

Similar to the response in two measured C-X-C chemokines, PHL cultures also show increases in both mRNA and protein expression of CCL4. Like CXCL10, CCL4 mRNA expression was increased in a dose-dependent manner, while increased protein expression occurred at all concentrations tested. Consistent with other cytokines, there were no changes in CCL4 expression in HepG2 cultures. Chemokines of the macrophage inflammatory protein 1 (MIP1) family are responsible for recruiting pro-inflammatory cells from the systemic circulation to a local site. It has been reported that IL-1β from monocyte conditioned medium was able to stimulate the production of CCL4 in HepG2 and Huh-7 human carcinoma cells lines.[32] Our results show an increase in IL-1β mRNA expression (data not shown) and CCL4 mRNA and protein expression in PHL cultures. Taken together, increases in IL-1β may be responsible for the increases seen in CCL4.

Interestingly, there were only slight increases in tumor necrosis factor alpha (TNFα) mRNA expression at intermediate Qdot doses. TNFα is recognized to be one of the most commonly expressed inflammatory cytokines. HMOX1 has been shown to block expression of TNFα, as well as IL-1β and MIP-1β, *via* the production of CO. The mechanism underlying this effect of TNFα has been shown to be mediated through MAP kinase-related pathways.[33] While this does not explain the failure of HMOX1 to block the expression of MIP-1β, HMOX-1 is thought to play a role in angiogenesis by interacting with vascular endothelial growth factor (VEGF).[34] Furthermore, CXCL10 can be modulated by HMOX-1 expression in renal tubular epithelial cells.[35] Thus, it is possible that TOPO-PMAT Qdot exposure could interfere with homeostatic balances of pro- and anti-angiogenic signaling as well as other chemokine pathways.[36]

Collectively, these results demonstrate that TOPO-PMAT Qdots elicit an inflammatory response in primary human liver cultures containing hepatocytes and a small population of Kupffer cells. The increase in gene expression and release of cytokines/chemokines measured suggest a pro-inflammatory macrophage phenotype (M1) *versus* the normally tolerogenic state of Kupffer cells (M2) which reside in the liver to process microbes from the intestinal tract.[37] While primary inflammatory cytokines (TNFα and IL-1β) are only slightly elevated, the robust increases in IL8 and CCL4 are suggestive of an altered hepatic state associated with chronic liver disease.[22]

CONCLUSIONS

In summary, our results show that TOPO-PMAT-coated CdSe Qdots do not exhibit significant overt cytotoxicity. However, secondary responses to TOPO-PMAT Qdots may result in a pro-inflammatory response within the liver. We saw an increase of pro-inflammatory chemokines/cytokines associated with immune cell recruitment in hepatitis, as well as cellular stress markers in PHL cultures, but not HepG2 cultures. While *in vivo* studies are important to investigate biological response to nanoparticles at the organ level, appropriate *in vitro* models containing relevant cell types have value for estimating tissue level responses. Further studies in primary liver cultures and *in vivo* mouse models are necessary to more thoroughly investigate the mechanism and relevance of this response. Also, the variability between various liver preparations illustrates the heterogeneity of the human population and reflects the importance of considering variable responses from different donors.

MATERIALS AND METHODS

Materials and Instruments. TOPO-coated CdSe/ZnS core/shell QDs (620 nm emission) were provided by Oceannanotech LLC as a gift (Springdale, AK). Poly(maleic anhydride-*alt*-tetradecene) was purchased from Sigma-Aldrich, Inc. (St. Louis, MO). A UV-2450 spectrophotometer (Shimadzu, Columbia, MD) and a Fluoromax4 fluorimeter (Horiba Jobin Yvon, Edison, NJ) were used to characterize the absorption and emission spectra of the modified QDs. A tabletop ultracentrifuge (Beckman TL120) was used for nanoparticle purification and isolation. The diameters of dry QDs were measured on a FEI Tecnai transmission electron microscope (FEI Corporate Headquarters, Hillsboro, OR) and a Zetasizer NanoZS size analyzer (Malvern, Worcestershire, UK).

Synthesis of Quantum Dots. TOPO-PMAT Qdots were synthesized as previously described.[2,27,38] Briefly, 40 mg of PMAT was mixed with 17.7 nmol of QDs in chloroform. The solvent was then allowed to slowly dry in air, leading to the formation a thin film of QD-PMAT complexes. The dried film was dissolved in 50 mM borate buffer (pH 8.5) with agitation or sonication. Free PMAT polymers (unbound polymers) were removed by 3 rounds of ultracentrifugation (50k rpm for 1 h each). Absorption and fluorescence emission spectra of the modified Qdots were measured on a UV-2450 spectrophotometer (Shimadzu,

Columbia, MD) and a Fluoromax4 spectrofluorometer (Horiba Jobin Yvon, Edison, NJ), respectively. A Zetasizer NanoZS size analyzer (Malvern, Worcestershire, UK) was used to measure the hydrodynamic diameter (12.7 ± 0.5 nM) and zeta-potential (−43 mV) of the Qdots.[27] Concentration determination of TOPO-PMAT Qdots was determined by absorption with a standard curve.

Cell Culture. HepG2 cells were obtained from ATCC (Manassas, GA) and cultured in MEM-α medium supplemented with 5% NuSerum (BD Biosciences, Bedford, MA), 100 IU/mL penicillin and 100 μg/mL streptomycin, and maintained in 5% CO_2/95% humidified air at 37 °C. Cells were plated in 35 mm tissue culture dishes at 5×10^5 cells/cm^2 and allowed to grow for 48 h prior to Qdot exposure. Qdots were suspended in medium and then sterile filtered with a 0.22 μM pore poly-vinylidene difluoride (PVDF) membrane (Millipore, Billerica, MA) prior to addition in cell cultures. PHL cell cultures were derived from viable human livers that were rejected for transplantation for various reasons. PHL cells were obtained from Dr. Steven Strom (University of Pittsburgh), through the NIH Liver Cell and Tissue Distribution System (LCTDS). All human subjects' proto-cols for organ collection were reviewed and approved by the University of Pittsburgh Internal Review Board. The use of these samples does not constitute human subjects research as de-termined by the University of Washington IRB. Isolation of human liver cells was performed as described previously.[16] PHL cells were maintained at 37 °C under 5% CO_2/95% humi-dified air on a rigid collagen substratum overlaid with Matrigel (BD Biociences, San Jose CA) in supplemented Williams E media as previously reported.[16] Previous studies have shown that the collagen/Matrigel "sandwich" culture decreases expression of cellular stress genes and increases the expression of biotrans-formation enzymes, as well as other genes associated with liver-specific function.[39] These conditions maintain albumin secre-tion for up to 10 days.[15] PHL cells were incubated for 24 h after receiving them to allow for recovery from shipment. The cells were then treated with Qdots or an equal volume of medium for 24 h at a range of doses (0−40 nM) prior to analysis.

Fluorescence Microscopy. Qdot uptake was evaluated by digital fluorescence imaging using a Nuance hyperspectral imaging camera (Cambridge Research, Inc., Hopkinton MA), mounted on a Nikon Optiphot microscope (Nikon USA, Melville, NY). After 24 h of incubation, medium containing Qdots was removed and cultures were washed 2× with PBS. Nuclei were then stained with cell-membrane-permeable Hoechst dye (HO33342), and fluorescence measurements were recorded. Two color digital images were obtained using UV excitation (365 nm) and blue emission (460 ± 5 nm band-pass filter) to detect Hoechst dye nuclear staining, and fluorescence emission was collected at 620 ± 5 nm band-pass filter for Qdot-specific fluorescence. Averaging time for imaging was held constant among treat-ments within each cell line. Tiff images were then exported to Metamorph software (Molecular Devices, Sunnyvale, CA) for further processing and quantitation.

MTT Assay. Cells were incubated with Qdots for 24 h in 24-well plates. Cellular viability was quantitated by a colorimetric method utilizing the metabolic dye 3-(4,5-dimethylthiazol-2-yl)-2,5 diphenyltetrazolium bromide (MTT).[40] MTT is reduced by mitochondrial dehydrogenases in metabolically active cells causing the development of an intracellular purple formazan precipitate that can be solubilized with DMSO and quantified by spectro-photometry. An aliquot of 50 μL of a 5 mg/mL solution of MTT was added to each well and incubated for 1 h at 37 °C. Subsequently, the medium containing Qdots and MTT solution was carefully removed and the formazan reaction product dissolved with DMSO (150 μL/well). Absorbance was read at 570 nm, and the results are expressed as percent viability relative to controls.

Measurement of Glutathione Levels. Total intracellular glu-tathione (GSH) levels were measured as described previously.[41] Briefly, cells were homogenized by incubation with Mammalian Purification Extraction Reagent (MPER; Thermo Fisher Scientific, Rockford, IL) as per the manufacturer's instructions. An aliquot was taken to measure the protein concentration, while a second aliquot was diluted (1:1) with 10% 5-sulfosalicylic acid (SSA). The SSA fraction was centrifuged at 12 000 rpm for 5 min at 4 °C and

the supernatant measured for GSH quantitation. Aliquots from the SSA fraction were added to a 96-well plate, and the pH was adjusted to 7.0 with 0.2 M N-ethylmorpholine/0.02 M KOH. Glutathione disulfide (GSSG) was reduced to GSH by adding 10 μL of 10 mM tris(2-carboxyethyl)phosphine hydrochloride (TCEP) for 15 min at room temperature. The pH was then adjusted to 12.5 using 0.5 N NaOH before derivatizing the samples with naphthalene dicarboxaldehyde (NDA; 0.5 mM) for 30 min. Lastly, the samples were analyzed on a spectro-fluorometric plate reader (λ_{EX} 472 and λ_{EM} 528 nm). The total amount of GSH in the sample was reported as nmol/mg protein by interpolating from a standard curve obtained by plotting known amounts of GSH incubated in the same experimental conditions. Protein levels were determined with the BCA re-agent (Pierce, Rockford, IL) per manufacturer's instructions.

Measurement of Cadmium. Quantum dots were prepared as previously mentioned by suspension in media and sterile filtered prior to centrifugation at 50 000g for 1 h at 4 °C (Beckman Ti 70.1 rotor; Beckman Instrumentation, Fullerton, CA). Cadmium levels were detected with ICP-MS utilizing a standard protocol (EPA 6020A).

RT-PCR. The steady-state mRNA levels of genes involved in cellular stress response (*MT1A*, *HMOX1*, *GCLC*, and *GCLM*) and inflammation (*TNF*α, *CXCL8*, *CCL4*, and *IL-1β*) were measured using quantitative real-time reverse transcriptase polymerase chain reaction (qRT-PCR). Following 24 h of treatment with Qdots, cells were lysed with the addition of TRIzol reagent (Invitrogen, Carlsbad, CA). RNA was extracted and purified utilizing standard phenol/chloroform extraction procedures. The quality of RNA was then measured electrophoretically by examining 18s and 28s band intensities utilizing an Agilent 2100 bioanalyzer (Agilent, Santa Clara, CA). Reverse transcription (RT) of 0.1−0.2 μg of total RNA was performed using oligo-dT 15 primer and SuperscriptII RNaseH (Gibco, Carlsbad, CA), follow-ing the manufacturer's instructions. Quantitative RT-PCR was performed using fluorogenic 5′ nuclease assays on an ABI PRISM 7900HT system (Applied Biosystems Inc., Foster City, CA).

Western Blotting. After treatment for 24 h, cells were rinsed 1× with PBS (RT) and the appropriate amount of MPER following manufacturer's instructions. One-half of the mixture was frozen at −80 °C in 10% SSA for GSH analysis. The remaining aliquot was centrifuged at 13 300g for 20 min to remove cell debris, and the supernatant was stored at −80 °C until analyzed. Equal amounts of soluble protein were resolved on a 4−12% gradient polyacrylamide gel (Nupage Bis/Tris) and then transferred to PVDF membranes (Millipore, Bedford MA). Membranes were probed for GCLC and GCLM (Franklin, 2003), HMOX1 (R&D Systems, Minneapolis MN), and β-actin (loading control).

Cytokine Detection by Luminex Bead Array. Medium from Qdot-treated hepatocytes was collected, centrifuged at 100g, and the supernatant was stored at −80 °C until being measured with the Luminex 200 system as specified by the manufacturer (Luminex, Austin, TX). These samples were subsequently tested in multiplex assays for the presence of TNFα, CXCL8, CCL4, and CXCL10 using polystyrene antibody bead kits (Biosource/Invitrogen) and the Luminex xMAP system.

Conflict of Interest: The authors declare no competing financial interest.

Supporting Information Available: Photomicrographs of dis-persion of TOPO-PMAT Qdots in William's E media, and in modified Eagle's medium with alpha modification (MEMα) supplemented with NuSerum, after 24 h at 37 °C. This material is available free of charge *via* the Internet at http://pubs.acs.org.

REFERENCES AND NOTES

1. Hu, X.; Gao, X. Silica−Polymer Dual Layer-Encapsulated Quantum Dots with Remarkable Stability. *ACS Nano* **2010**, *4*, 6080–6086.

2. Bagalkot, V.; Gao, X. siRNA-Aptamer Chimeras on Nanoparticles: Preserving Targeting Functionality for Effective Gene Silencing. *ACS Nano* **2011**, *5*, 8131–8139.

3. Smith, A.; Duan, H.; Mohs, A.; Nie, S. Bioconjugated Quantum Dots for *In Vivo* Molecular and Cellular Imaging. *Adv. Drug Delivery Rev.* **2008**, *60*, 1226–1240.

4. Gao, X.; Cui, Y.; Levenson, R. M.; Chung, L. W. K.; Nie, S. *In Vivo* Cancer Targeting and Imaging with Semiconductor Quantum Dots. *Nat. Biotechnol.* **2004**, *22*, 969–976.

5. Ye, L.; Yong, K.-T.; Liu, L.; Roy, I.; Hu, R.; Zhu, J.; Cai, H.; Law, W.-C.; Liu, J.; Wang, K.; *et al.* A Pilot Study in Non-Human Primates Shows No Adverse Response to Intravenous Injection of Quantum Dots. *Nat. Nanotechnol.* **2012**, DOI: 10.1038/nnano.2012.74.

6. Derfus, A. M.; Chan, W. C. W.; Bhatia, S. N. Probing the Cytotoxicity of Semiconductor Quantum Dots. *Nano Lett.* **2004**, *4*, 11–18.

7. Kirchner, C.; Liedl, T.; Kudera, S.; Pellegrino, T.; Muñoz Javier, A.; Gaub, H. E.; Stölzle, S.; Fertig, N.; Parak, W. J. Cytotoxicity of Colloidal CdSe and CdSe/ZnS Nanoparticles. *Nano Lett.* **2005**, *5*, 331–338.

8. Su, Y.; He, Y.; Lu, H.; Sai, L.; Li, Q.; Li, W.; Wang, L.; Shen, P.; Huang, Q.; Fan, C. The Cytotoxicity of Cadmium Based, Aqueous Phase-Synthesized, Quantum Dots and Its Modulation by Surface Coating. *Biomaterials* **2009**, *30*, 19–25.

9. Su, Y.; Hu, M.; Fan, C.; He, Y.; Li, Q.; Li, W.; Wang, L.-H.; Shen, P.; Huang, Q. The Cytotoxicity of CdTe Quantum Dots and the Relative Contributions from Released Cadmium Ions and Nanoparticle Properties. *Biomaterials* **2010**, *31*, 4829–4834.

10. Shiohara, A.; Hoshino, A.; Hanaki, K.; Suzuki, K.; Yamamoto, K. On the Cyto-toxicity Caused by Quantum Dots. *Microbiol. Immunol.* **2004**, *48*, 669–675.

11. Chen, N.; He, Y.; Su, Y.; Li, X.; Huang, Q.; Wang, H.; Zhang, X.; Tai, R.; Fan, C. The Cytotoxicity of Cadmium-Based Quantum Dots. *Biomaterials* **2012**, *33*, 1238–1244.

12. Fischer, H. C.; Hauck, T. S.; Gómez-Aristizábal, A.; Chan, W. C. W. Exploring Primary Liver Macrophages for Studying Quantum Dot Interactions with Biological Systems. *Adv. Mater.* **2010**, *22*, 2520–2524.

13. Diagaradjane, P.; Deorukhkar, A.; Gelovani, J. G.; Maru, D. M.; Krishnan, S. Gadolinium Chloride Augments Tumor-Specific Imaging of Targeted Quantum Dots *in Vivo*. *ACS Nano* **2010**, *4*, 4131–4141.

14. Hewitt, N. J.; Lechón, M. J. G.; Houston, J. B.; Hallifax, D.; Brown, H. S.; Maurel, P.; Kenna, J. G.; Gustavsson, L.; Lohmann, C.; Skonberg, C.; *et al.* Primary Hepatocytes: Current Understanding of the Regulation of Metabolic Enzymes and Transporter Proteins, and Pharmaceutical Practice for the Use of Hepatocytes in Metabolism, Enzyme Induction, Transporter, Clearance, and Hepatotoxicity Studies. *Drug Metab. Rev.* **2007**, *39*, 159–234.

15. Sellaro, T. L.; Ranade, A.; Faulk, D. M.; McCabe, G. P.; Dorko, K.; Badylak, S. F.; Strom, S. C. Maintenance of Human Hepatocyte Function *in Vitro* by Liver-Derived Extracellular Matrix Gels. *Tissue Eng., Part A* **2010**, *16*, 1075–1082.

16. Gross-Steinmeyer, K.; Stapleton, P. L.; Tracy, J. H.; Bammler, T. K.; Lehman, T.; Strom, S. C.; Eaton, D. L. Influence of Matrigel-Overlay on Constitutive and Inducible Expression of Nine Genes Encoding Drug-Metabolizing Enzymes in Primary Human Hepatocytes. *Xenobiotica* **2005**, *35*, 419–438.

17. Tuschl, G.; Hrach, J.; Walter, Y.; Hewitt, P. G.; Mueller, S. O. Serum-Free Collagen Sandwich Cultures of Adult Rat Hepatocytes Maintain Liver-like Properties Long Term: A Valuable Model for *In Vitro* Toxicity and Drug−Drug Interaction Studies. *Chem.-Biol. Interact.* **2009**, *181*, 124–137.

18. Tu, Z.; Bozorgzadeh, A.; Crispe, I. N.; Orloff, M. S. The Activation State of Human Intrahepatic Lymphocytes. *Clin. Exp. Immunol.* **2007**, *149*, 186–193.

19. Cho, S. J.; Maysinger, D.; Jain, M.; Röder, B.; Hackbarth, S.; Winnik, F. M. Long-Term Exposure to CdTe Quantum Dots Causes Functional Impairments in Live Cells. *Langmuir* **2007**, *23*, 1974–1980.

20. Eaton, D. L.; Stacey, N. H.; Wong, K. L.; Klaassen, C. D. Dose-Response Effects of Various Metal Ions on Rat Liver Metallothionein, Glutathione, Heme Oxygenase, and Cytochrome P-450. *Toxicol. Appl. Pharmacol.* **1980**, *55*, 393–402.

21. Tchounwou, P. B.; Ishaque, A. B.; Schneider, J. Cytotoxicity and Transcriptional Activation of Stress Genes in Human Liver Carcinoma Cells (HepG2) Exposed to Cadmium Chloride. *Mol. Cell. Biochem.* **2001**, *222*, 21–28.

22. Zimmermann, H. W.; Seidler, S.; Gassler, N.; Nattermann, J.; Luedde, T.; Trautwein, C.; Tacke, F. Interleukin-8 Is Activated in Patients with Chronic Liver Diseases and Associated with Hepatic Macrophage Accumulation in Human Liver Fibrosis. *PLoS ONE* **2011**, *6*, e21381.

23. Dudley, R. E.; Klaassen, C. D. Changes in Hepatic Glutathione Concentration Modify Cadmium-Induced Hepatotoxicity. *Toxicol. Appl. Pharmacol.* **1984**, *72*, 530–538.

24. Weldy, C. S.; Wilkerson, H.-W.; Larson, T. V.; Stewart, J. A.; Kavanagh, T. J. Diesel Particulate Exposed Macrophages Alter Endothelial Cell Expression of eNOS, iNOS, MCP1, and Glutathione Synthesis Genes. *Toxicol. In Vitro* **2011**, *25*, 2064–2073.

25. Krejsa, C. M.; Franklin, C. C.; White, C. C.; Ledbetter, J. A.; Schieven, G. L.; Kavanagh, T. J. Rapid Activation of Glutamate Cysteine Ligase Following Oxidative Stress. *J. Biol. Chem.* **2010**, *285*, 16116–16124.

26. Yao, P.; Hao, L.; Nussler, N.; Lehmann, A.; Song, F.; Zhao, J.; Neuhaus, P.; Liu, L.; Nussler, A. The Protective Role of HO-1 and Its Generated Products (CO, Bilirubin, and Fe) in Ethanol-Induced Human Hepatocyte Damage. *Am. J. Physiol.* **2009**, *296*, G1318–23.

27. McConnachie, L. A.; White, C. C.; Botta, D.; Zadworny, M. E.; Cox, D. P.; Beyer, R. P.; Hu, X.; Eaton, D. L.; Gao, X.; Kavanagh, T. J. Heme Oxygenase Expression as a Biomarker of Exposure to Amphiphilic Polymer-Coated CdSe/ZnS Quantum Dots. *Nanotoxicology* **2012**, DOI: 10.3109/17435390.2011.648224.

28. Otterbein, L. E.; Soares, M. P.; Yamashita, K.; Bach, F. H. Heme Oxygenase-1: Unleashing the Protective Properties of Heme. *Trends Immunol.* **2003**, *24*, 449–455.

29. Fischer, H. C.; Liu, L.; Pang, K. S.; Chan, W. C. W. Pharmacokinetics of Nanoscale Quantum Dots: *In Vivo* Distribution, Sequestration, and Clearance in the Rat. *Adv. Funct. Mater.* **2006**, *16*, 1299–1305.

30. Oo, Y. H.; Adams, D. H. The Role of Chemokines in the Recruitment of Lymphocytes to the Liver. *J. Autoimmun.* **2010**, *34*, 45–54.

31. Hintermann, E.; Bayer, M.; Pfeilschifter, J. M.; Luster, A. D.; Christen, U. CXCL10 Promotes Liver Fibrosis by Prevention of NK Cell Mediated Hepatic Stellate Cell Inactivation. *J. Autoimmun.* **2010**, *35*, 424–435.

32. Zhang, T.; Guo, C. J.; Li, Y.; Douglas, S. D.; Qi, X. X.; Song, L.; Ho, W. Z. Interleukin-1 [Beta] Induces Macrophage Inflammatory Protein-1 [Beta] Expression in Human Hepatocytes. *Cell. Immunol.* **2003**, *226*, 45–53.

33. Otterbein, L. E.; Bach, F. H.; Alam, J.; Soares, M.; Tao, Lu, H.; Wysk, M.; Davis, R. J.; Flavell, R. A.; Choi, A. M. Carbon Monoxide Has Anti-Inflammatory Effects Involving the Mitogen-Activated Protein Kinase Pathway. *Nat. Med.* **2000**, *6*, 422–428.

34. Dulak, J.; Łoboda, A.; Zagórska, A.; Józkowicz, A. Complex Role of Heme Oxygenase-1 in Angiogenesis. *Antioxid. Redox Signal.* **2004**, *6*, 858–866.

35. Datta, D.; Dormond, O.; Basu, A.; Briscoe, D. M.; Pal, S. Heme Oxygenase-1 Modulates the Expression of the Anti-Angiogenic Chemokine CXCL-10 in Renal Tubular Epithelial Cells. *Am. J. Physiol. Renal Physiol.* **2007**, *293*, F1222–30.

36. Kanakiriya, S. K. R.; Croatt, A. J.; Haggard, J. J.; Ingelfinger, J. R.; Tang, S.-S.; Alam, J.; Nath, K. A. Heme: A Novel Inducer of MCP-1 through HO-Dependent and HO-Independent Mechanisms. *Am. J. Physiol. Renal Physiol.* **2003**, *284*, F546–54.

37. Callery, M. P.; Mangino, M. J.; Flye, M. W. Arginine-Specific Suppression of Mixed Lymphocyte Culture Reactivity by Kupffer Cells—A Basis of Portal Venous Tolerance. *Transplantation* **1991**, *51*, 1076–1080.

38. Pellegrino, T.; Manna, L.; Kudera, S.; Liedl, T.; Koktysh, D.; Rogach, A. L.; Keller, S.; Rädler, J.; Natile, G.; Parak, W. J. Hydrophobic Nanocrystals Coated with an Amphiphilic Polymer Shell: A General Route to Water Soluble Nanocrystals. *Nano Lett.* **2004**, *4*, 703–707.

39. Page, J. L.; Johnson, M. C.; Olsavsky, K. M.; Strom, S. C.; Zarbl, H.; Omiecinski, C. J. Gene Expression Profiling of Extracellular Matrix as an Effector of Human Hepatocyte Phenotype in Primary Cell Culture. *Toxicol. Sci.* **2007**, *97*, 384–397.

40. Mosmann, T. Rapid Colorimetric Assay for Cellular Growth and Survival: Application to Proliferation and Cytotoxicity Assays. *J. Immunol. Methods* **1983**, *65*, 55–63.

41. White, C. Fluorescence-Based Microtiter Plate Assay for Glutamate−Cysteine Ligase Activity. *Anal. Biochem.* **2003**, *318*, 175–180.